Submillimetre Formwork: 3D-Printed Plastic Formwork for Concrete Elements

Andrei Jipa
Digital Building Technologies, Institute of Technology in Architecture, ETH Zürich

Mathias Bernhard
Digital Building Technologies, Institute of Technology in Architecture, ETH Zürich

Benjamin Dillenburger
Digital Building Technologies, Institute of Technology in Architecture, ETH Zürich

1 ABSTRACT

Submillimetre Formwork is a novel method for fabricating geometrically complex concrete parts with 3D-printed plastic formwork (fig. 1). This research investigates how 3D printing can be used to fabricate submillimeter-thin formwork. To achieve this, computational methods for optimizing the fabrication speed of formwork with plastic deposition 3D printing are developed, as well as methods to stabilize the minimal formwork during the casting process. Without any coating and post-processing steps, the plastic formwork is easily removable, recyclable and bio-degradable. The implications of *Submillimetre Formwork* are a considerable material reduction, faster off-site fabrication time for the formwork, ease of transportation to site, ease of on-site assembly, and unprecedented design opportunities for free form and highly detailed concrete components.

2 INTRODUCTION

With more than 10 billion tons produced each year, concrete is by far one of the most used materials in the world, second only to water (Olivier, Janssens-Maenhout, Muntean, & Peters 2016). Concrete is ubiquitous in the building industry due to its versatility, wide availability of raw materials, and low embodied energy. It is favored by engineers because it has excellent structural properties, and it is celebrated by architects because it can be cast into any conceivable shape.

But in order for concrete to materialize a shape, it needs a formwork to be cast in, a mold to be sprayed on, or a die to be extruded through. The excellent geometric potential of concrete is therefore limited by the ability to fabricate the necessary formwork.

> *Although reinforced concrete has been used for over a hundred years and with increasing interest during the last decades, few of its properties and potentialities have been fully exploited so far. Apart from the unconquerable inertia of our own minds, which do not seem to be able to adopt freely any new ideas, the main cause of this delay is a trivial technicality: the need to prepare wooden frames. (Nervi 1956)*

For concrete construction, formwork accounts for a significant amount of resources, both in terms of material costs and labor (fig. 2). In particular, for free-form, non-standard parts, formwork resources can represent more than 60% of the whole construction, more than

Figure 1: Prototype for an architectural concrete element cast in Submillimetre Formwork. - DBT, ETH Zürich, 2017

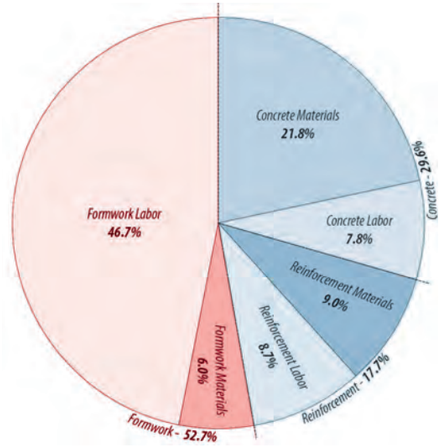

Figure 2: Breakup of costs in concrete production. On average, formwork accounts for roughly half the resources in terms of both labor and materials (Oesterle, Vansteenkiste, and Mirjan 2012).

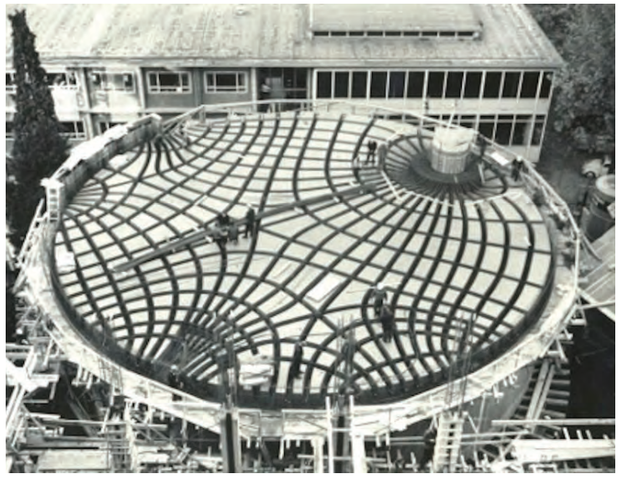

Figure 3: Formwork represented 80% of the construction costs for the slab of the Zoology Lecture Hall of the University of Freiburg, designed by Hans Dieter Hecker in 1969 (Antony et al. 2014).

concrete and reinforcement combined (fig. 3).

The elevated cost of non-standard formwork compared to the low cost of raw materials discourages complex geometries that efficiently distribute material. Geometrical simplicity is preferred over optimal material use because materials are cheap and custom formworks are expensive.

Given the significant importance of formwork in concrete construction, the aim of this research is to minimize the amount of material and labor used for fabricating formwork. The objective is to develop an efficient, automated fabrication method based on 3D printing which can be used for making formwork for large-scale, complex concrete components. This can have further positive effects on: the sustainability of formwork; speeding up formwork fabrication off-site; reducing the cost of transportation; streamlining assembly on site; and facilitating removal and reusability after casting.

Yet the most significant advantage of 3D-printed formworks is their potential to enable complex topologies to be cast in concrete, which can have further indirect implications:

- Considerable material reduction through computational topology optimization algorithms, which result in complex geometries (Jipa et al. 2016).
- Integration of additional functionality, such as surfaces with acoustic properties, thermal activation, insulation, and enclosures for building services.
- Smart integration of construction and assembly logics that streamline on-site fabrication, such as interlocking connections and referencing systems.
- New design possibilities for free-form geometries and high-resolution ornamental surface articulation (Dillenburger and Hansmeyer 2013).

Production of formwork for non-standard concrete elements is done in practice by robotic hot wire cutting or CNC milling of foam blocks (Søndergaard, Amir, and Knauss 2013). Lightweight formwork can also be produced with fabric (Veenendaal, West, and Block 2011). However, these approaches are resource-intensive as regards necessary time and labor (milling tools are slow and fabrics require extensive patterning) and have limitations regarding the geometries that can be produced (e.g. no undercuts for milling, and only smooth, anticlastic surfaces for fabrics).

3 3D-PRINTED FORMWORK

To overcome these limitations, different 3D-printing technologies have already been proposed for formwork (fig. 4). The architect and researcher Philippe Morel of EZCT has experimented with two different technologies to 3D print formwork for concrete. Clay robo-casting produced a rough result, inheriting the coarse layers of the extrusion process. With binder jetting, he created a three-dimensional triangulated truss structure cast in concrete to demonstrate this material's load bearing capacities. The binder-jetted half shells are infiltrated with epoxy resin and assembled to form the hollow tubular mold prior to being cast. The structure has a very smooth surface quality; however, it lacks reinforcement. Additionally, formwork removal limits to some extent the geometric freedom (Gosselin et al. 2016).

A jump in scale and resolution was made with the realization of the Swiss pavilion for the 2016 Architecture Biennale in Venice. "Incidental Space," designed by Christian Kerez, is a 9m-long and 6m-high room enclosed by a 2-cm-thin shell of polymer fiber reinforced shotcrete. Around a third of the formwork parts were binder jetted in sandstone and infiltrated with a release agent. No other known fabrication method would have allowed for the production of this level of detail (Dillenburger 2016).

A further precedent of binder-jetted formwork comes from ETH Zürich, where a 1.8m^2 topologically optimized slab was fabricated using ultra-high-performance fiber-reinforced concrete (UHPFRC) cast in a 9mm-thick sandstone 3D-printed shell. This showed how the complex topologies resulting from computational optimization algorithms can be fabricated to considerably reduce material in load-bearing components (Aghaei-Meibodi et al. 2017).

In contrast with the first two examples which use binder jetting, Brian Peters from Kent State University tested and patented fused deposition modelling (FDM) for fabricating formwork (Peters 2014). Peters discusses small-scale horizontal elements, and his research shows that there are inherent characteristics of FDM 3D printing that need to be addressed in order to make this technology feasible for large-scale fabrication. Scaling up and applying this process to vertical components such as walls and columns is challenging due to the hydrostatic pressure exerted by the concrete on the formwork.

The research question posed by *Submillimetre Formwork* is how large-scale, geometrically complex structural concrete parts can be produced with minimal FDM 3D-printed formwork.

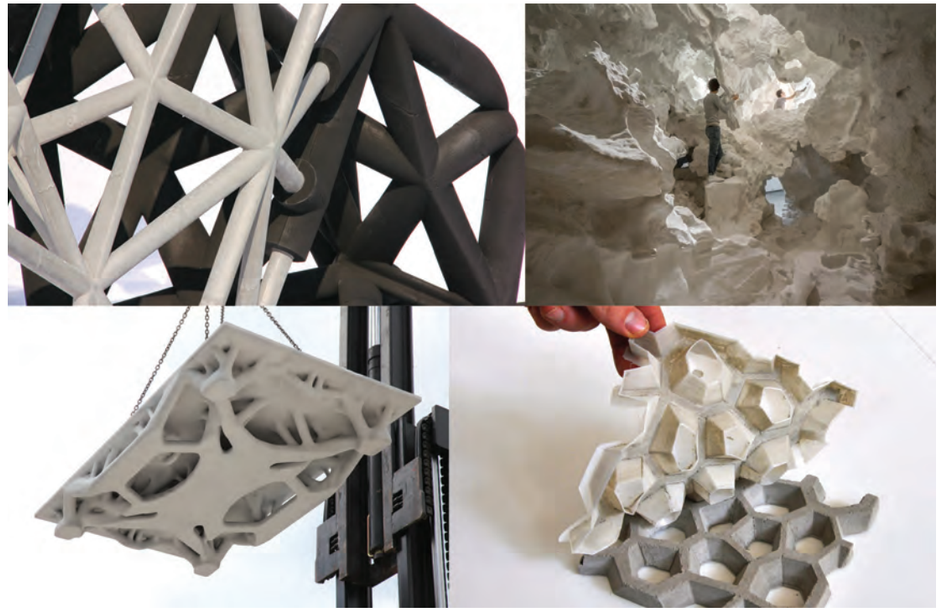

Figure 4: Precedents of 3D-printed formwork for concrete, clockwise from top left: Philippe Morel, EZCT 3D-Printed Formwork, 2014; Christian Kerez, Incidental Space, 2016; DBT, The Smart Take from the Strong, 2017; and Brian Peters, Additive Formwork, 2014.

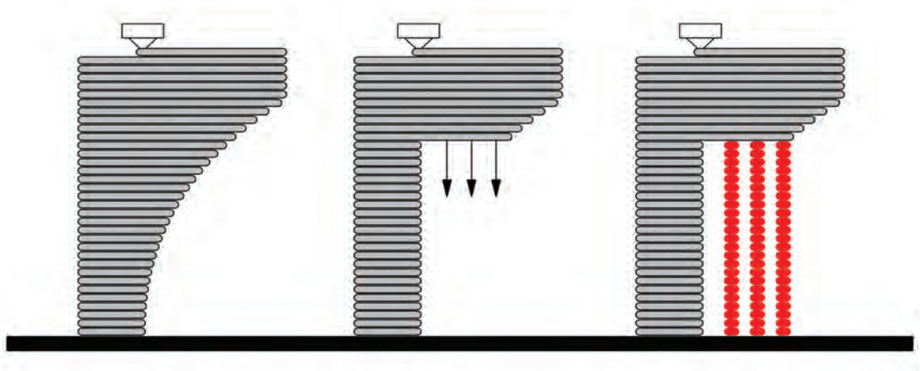

Figure 5: The FDM fabrication process requires auxiliary support structures (in red) for certain geometric features, such as overhangs and cantilevers. - DBT, ETH Zürich, 2017.

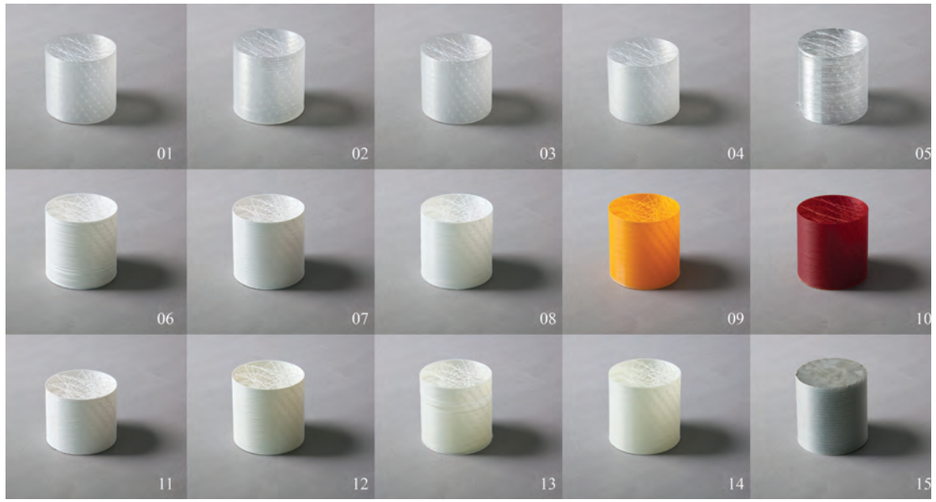

Figure 6: Different thermoplastics tested for finding a balance between printing speed, quality, and shrinkage. From the highest printing speeds achieved to the lowest: natural polylactic acid (01); natural polylactic acid/ polyhydroxyalkanoate blends (02–04), polyethylene terephthalate glycol-modified (05 and 06), polylactic acid with pigments (07–10), polyvinyl alcohol (11), biodegradable plastic Green-Tec™ (12–15). - DBT, ETH Zürich, 2017

4 METHODS

FDM is a widely available 3D printing technology in which molten material is extruded and hardens immediately after the deposition. The deposition happens in consecutive horizontal layers which are generated as slices through a digital model of the part to be fabricated. Despite some fabrication limitations—such as the inability to produce unsupported cantilevers (fig. 5)—FDM is unique among the different 3D-printing technologies for its capability of producing large-scale freestanding parts with very thin geometric features, such as walls as thin as 0.4 mm.

Because of the nature of the FDM process—where the build material solidifies and cools down quickly—a limitation of this technology is determined by the dimensional inaccuracy caused by uneven shrinkage during thermal contraction. Shrinkage is a function of the total volume of plastic:

$dV = \mathbf{V}_0 \, ß \, dt$
where dV = shrinkage in m^3
V_0 = initial volume of the formwork in m^3
ß = volumetric thermal coefficient of PLA in $°C^{-1}$
dt = temperature variation in °C.

The overall time necessary for the 3D print is also a function of the volume of formwork:

$t = \mathbf{V}/Q$
where t = 3D printing time in s
V = total volume of the formwork in m^3
Q = volumetric flow rate of the 3D print in m^3/s.

By reducing the total volume of formwork material to the thinnest skin possible, both the 3D printing time and thermal shrinkage are reduced to a minimum. This section discusses how the plastic 3D printing and the concrete casting processes can be optimized to enable the fabrication of *Submillimetre Formwork*.

4.1 3D-Printed Plastics for Formwork

FDM is a relatively slow 3D printing process, usually able to produce volumetric flowrates of 15 cm^3/hour and resolve 0.1 mm features. With well-tuned machines, flowrates as high as 100 cm^3/hour can be reached, but this has a negative impact on the resolving power, which increases to 0.2 mm.

A critical factor in achieving such high flowrates is the material used. FDM can extrude a wide variety of plastics (biodegradable, water-soluble, fiber-reinforced, flexible, conductive, low-shrinkage, bioplastics, etc.). In order to achieve a balance between fabrication speed, quality, and shrinkage, different materials were tested, and finally translucent polylactic acid (PLA) was selected for its versatility and low shrinkage factor (fig. 6).

While flowrates of PLA can be further increased through mechanical improvements of the hardware, the focus of this research is to speed up the 3D printing process on the software side, by generating an optimal tool path that controls the movements of the 3D printer tool head.

4.2 Optimized 3D Printing Tool Paths

Tool paths are generated from horizontal slices through a CAD model of the part to be 3D-printed. A custom slicing tool was developed for optimizing the travel distances between the different contours in each horizontal slice. The contours are sorted with an efficient algorithm that minimizes the distances between consecutive contours (fig. 7). In order to compute this optimization problem, each layer is interpreted as a complete weighted graph, where the graph nodes are contours and the graph weights are

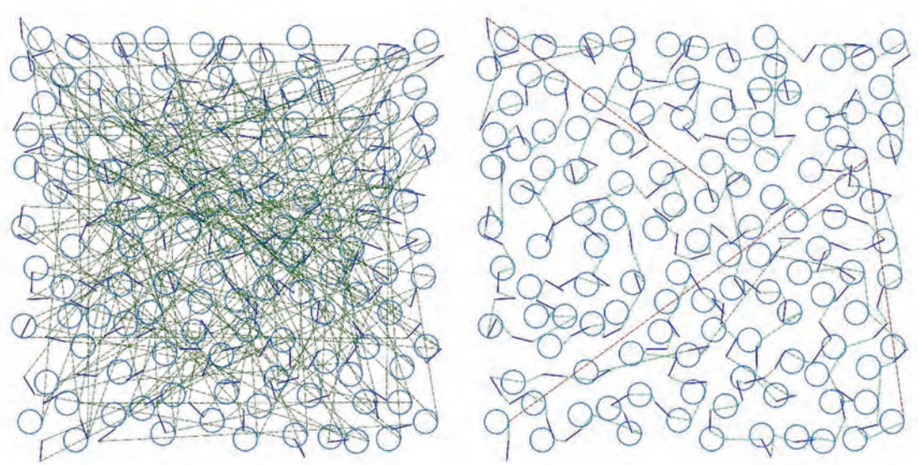

Figure 7: A slice through a CAD model with 100 line segments and 100 circles as contours. In a random order, this configuration generates a very long, inefficient tool path (left). The NNA arranges the 200 contours in an order that minimizes distances between consecutive contours (right). - DBT, ETH Zürich, 2017

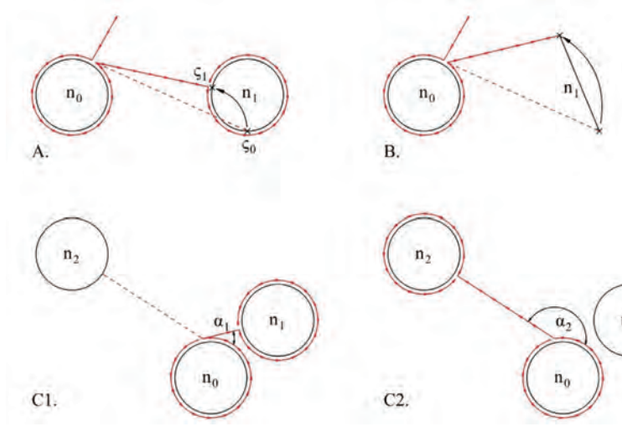

*Figure 8: Additional features of NNA. The tool-head first prints contour n0. When traveling to n1, the algorithm can: A) adjust the starting point **α** of closed contours; B) flip open contours; and C) calculate the loss in speed due to direction changes. Angles **α**1 for contour n1 and **α**2 for n2 are factored in the weight of each node. - DBT, ETH Zürich, 2017*

distances between contours. The problem is a variant of the classic 'travelling salesman' algorithm where the shortest toolpath (i.e. minimum-weight Hamilton circuit) has to be computed for the given graph (Lin and Kernighan 1973). To compute the shortest toolpath, a heuristic method is used, the nearest neighbor algorithm (NNA).

Calculating and comparing all the possible tool path variations with a brute force algorithm is impractical even for graphs with as little as 12 nodes. With the NNA heuristic, the search can be performed in linear time; however, the global optimal solution may be missed because of the greedy approach of the algorithm which relies on finding the local optimum at each step. Nevertheless, the NNA offers a good compromise between computation time and optimization.

For calculating the tool path, specific features were added to the generic form of the NNA:

- For each graph node that is a closed contour, the seam can be adjusted along the contour in order to find the shortest path at the current step (fig. 8A).
- For each graph node that is an open contour, both ends are compared in order to find the shortest travel distance at the current step, and the direction of the contour can be reversed (fig.8B).
- The cost function contains a factor p that takes into account the attack angle **α** between the incoming and outgoing direction of the tool head:

$p = 2 \cdot (1 - \mathbf{\alpha} / \mathbf{\pi}) \cdot (v_{max} - j) / a_{max}$
where p = penalty factor
α = change in direction in radians
v_{max} = feed rate of the tool head in mm/s
a_{max} = maximum acceleration of the tool head in mm/s^2
j = jerk federate of the tool head in mm/s.

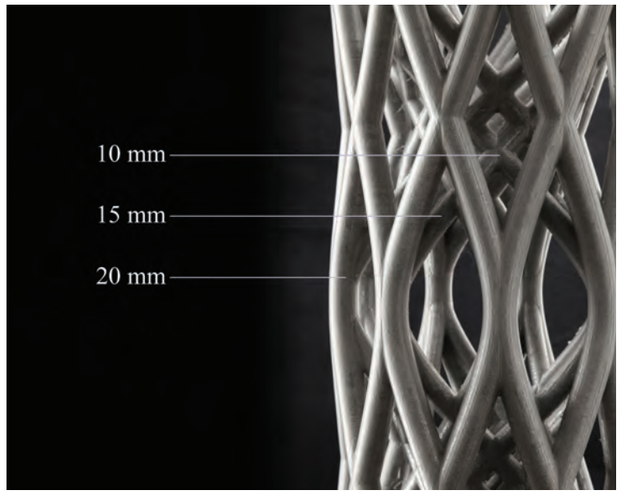

Figure 9: Concrete prototype using 3D-printed formwork displaying micro-tubular structures as small as 10 mm in diameter. - DBT, ETH Zürich, 2017

The factor p accounts for the fact that the tool head has to slow down more to negotiate tighter changes in direction. Negative and positive acceleration times have to be taken into consideration when calculating the total weight of the Hamilton circuit (fig. 8C).

4.3 Concrete Casting in Submillimetre Formwork

Ultra-high-performance fiber-reinforced concrete (UHPFRC) with 10-mm-long steel fibers was used (Aghaei-Meibodi et al. 2017). This satisfied the necessary rheological requirements to flow through the tubular geometric features as thin as 10 mm in diameter used in a series of prototypes (fig. 9).

The early prototypes revealed that one of the critical issues related to concrete casting is the buildup of hydrostatic pressure. The hydrostatic pressure is the maximum stress that is uniformly exerted by the concrete on the thin formwork. Hydrostatic pressure is only dependent on the density of UHPFRC and the depth of the cast:

$$p = \rho \cdot g \cdot h$$

where p = hydrostatic pressure in N/m^2
ρ = density of concrete in kg/m^3
g = gravitational acceleration in m/s^2
h = depth of the cast UHPFRC column in m.

The very thin PLA formwork is unable to withstand the hydrostatic pressure of the dense UHPFRC (ρ ~ 2,350 kg/m^3) for depths larger than circa-100 mm. The breaks in the formwork generally happen along the contact surface between consecutive 3D-printed layers, where there is a weak interface and lower tensile strength. In order to overcome this, several strategies have successfully been tested:

- Submerging the formwork in a bed of sand. The sand acts with a counter-pressure on the formwork that cancels out the hydrostatic pressure from the UHPFRC. Breaks are also neutralized by the sand, which consolidates the part locally and prevents further concrete leaks.
- Submerging the formwork progressively under water. This method also provides a counter-pressure on the outside of the form but has the advantage of keeping the casting process visible throughout. In combination with the transparent PLA, this is an important tool for monitoring the casting process for very challenging, thin geometric features (fig. 10).
- Coating the formwork with organic resins to increase its strength. Clear epoxy or polyester resins have been used to make the formwork waterproof, in addition to the two methods illustrated above.

Following the concrete casting, the PLA formwork provides the perfect enclosure for concrete curing, preventing the development of cracks due to water loss. Forty-eight hours after casting, the concrete is stable enough for removal of the formwork. A heat gun is used to supply moderate heat (~200°C), and the PLA peels off of the concrete on its own (fig. 11). After the removal, the uncoated PLA can be combusted, composted, or recycled.

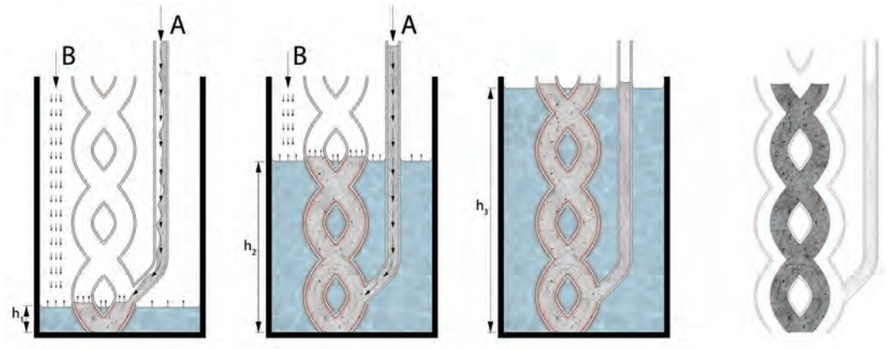

Figure 10: Step-by-step diagram showing the simultaneous infill of concrete through the bottom of the formwork (A) and of counter-pressure material (B – sand or water). The final step consists of the removal of the formwork and casting inlet. - DBT, ETH Zürich, 2017

Ongoing research is investigating alternative methods for the formwork removal, such as using polyvinyl alcohol as a 3D printing material. This can be removed easily because it is water-soluble, but the interaction with the hydration process of concrete needs to be tested further.

5 RESULTS

The method presented above optimizes fabrication times through a custom tool-path generation algorithm for 3D printing. Several commercial slicer tools do exist, but they produce tool paths that take at least twice as long to be 3D-printed (fig. 12).

Using such a thin shell as concrete formwork presents a number of challenges. Apart from the thermal shrinkage and fabrication speed, the research so far has identified challenges where further investigation is needed:

- The focus so far has been on parts which fit the size of a 3D printer. In order to fabricate larger parts, strategies for segmentation and connection need to be considered.
- Rheological limitations of concrete and fabrication limitations of FDM (fig. 5) have been identified empirically. A shape optimization process could address the limitations of the two processes and integrate geometric adjustments that make fabrication possible.

Figure 11: Concrete component displaying high-resolution texture (left) after the Submillimetre plastic formwork has been removed (right). - DBT, ETH Zürich, 2017

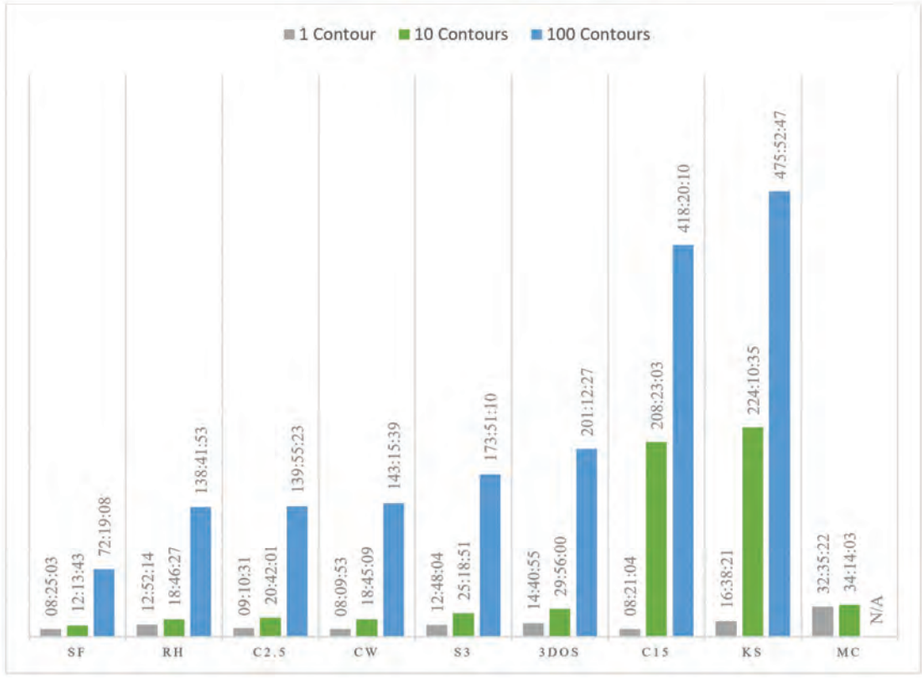

Figure 12: Comparison of printing times (in hours:minutes:seconds) of tool paths generated with different commercial slicers. Three different digital models with 1, 10, and 100 contours each were used for benchmarking. The printing time improvement for the custom slicer developed for Submillimetre Formwork (SF) is significant, especially for the model with 100 contours, where the fabrication is at least 50% faster compared to Repetier Host 2.0.1 (RH), Cura 2.5x64 (C2.5), Craftware 1.14 (CW), Slic3r 1.2.9 (S3), 3DPrinterOS.com (3DOS), Cura 15.04 (C15), KissSlicer 1.5x64 (KS) and MatterControl 1.4 (MC). - DBT, ETH Zürich, 2017

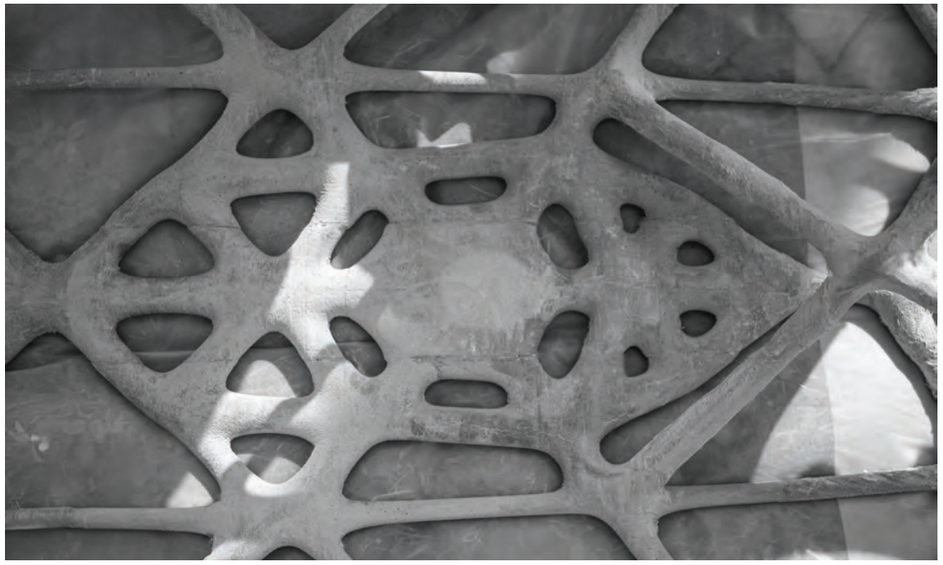

Figure 13: Load-bearing spatial concrete element cast in discretized Submillimetre Formwork. - DBT, ETH Zürich, 2017

- The structural performance of the components needs to be tested. Of particular interest is the orientation of the steel fibers in the intricate narrow tubes. Computed tomography coupled with computational fluid dynamics simulation could give some insight in this regard.

6 OUTLOOK

The next step in the research is to address the challenge of further scaling this fabrication process up. In order to investigate this, a four-meter-long, load-bearing spatial element was designed, optimized for a complex load case, and is being fabricated with the proposed method (fig. 13). This method opens new design possibilities for building elements with functional inner porosity, intricate surface qualities for functional or ornamental purposes, and integrated assembly logic.

7 CONCLUSION

Submillimetre Formwork relies on using 3D printing only for a minimal skin that is enough to ensure the complex shape of a concrete component. The stability of the fragile formwork during casting is provided by an ordinary material such as sand or water that does not require digital fabrication, thus using the precious fabrication process only where it is strictly needed to precisely define the shape (fig. 14).

It has been shown that for producing complex, free-form, and non-standard concrete elements, *Submillimetre Formwork* offers a novel, economical alternative, or even the only possible solution for the fabrication of certain geometric features. The novelty is twofold: on the one hand, an optimized 3D printing process for the formwork, and, on the other hand, a casting process that is suitable for such fragile formwork shells. FDM enables the full geometric and structural potential of fiber-reinforced concrete and promises a more sustainable construction process with no waste material, an easier on-site assembly with lightweight formwork, and a greater design freedom for concrete elements.

8 REFERENCES

Aghaei-Meibodi, M., M. Bernhard, A. Jipa, and B. Dillenburger. 2017. "The Smart Takes from the Strong." Paper presented at the Fabricate 2017: Rethinking Design and Construction, University of Stuttgart, Germany, April 6–8, 2017.

Antony, F., R. Grießhammer, T. Speck, and O. Speck. 2014. "Sustainability Assessment of a Lightweight Biomimetic Ceiling Structure." *Bioinspiration & Biomimetics,* 9 (1), 016013.

Dillenburger, B. 2016. "Incidental Space" im Schweizer Pavillon. TEC21 (23/2016).

Dillenburger, B., and M. Hansmeyer. (2013). "The Resolution of Architecture in the Digital Age." Paper presented at the International Conference on Computer-Aided Architectural Design Futures.

Gosselin, C., R. Duballet, P. Roux, N. Gaudillière, J. Dirrenberger, and P. Morel. 2016. "Large-Scale 3D Printing of Ultra-High Performance Concrete—A New Processing Route for Architects and Builders." *Materials & Design* 100, 102–109.

Figure 14: Prototype for an architectural concrete element cast in Submillimetre Formwork. - DBT, ETH Zürich, 2017.

Jipa, A., M. Bernhard, B. Dillenburger, and M. Aghaei-Meibodi, M. 2016. "3D-Printed Stay-in-Place Formwork for Topologically Optimized Concrete Slabs." Paper presented at the 2016 TxA Emerging Design + Technology, San Antonio, Texas, November 3–4, 2016.

Lin, S., and B. W. Kernighan. 1973. "An Effective Heuristic Algorithm for the Traveling-Salesman Problem." *Operations Research*, 21 (2), 498–516.

Nervi, P. L. 1956. *Structures.* New York: FW Dodge Corp.

Oesterle, S., A. Vansteenkiste, and A. Mirjan. 2012. "Zero Waste Free-Form Formwork." Paper presented at the Proceedings of the Second International Conference on Flexible Formwork, ICFF. CICM and University of Bath, Department of Architecture and Civil Engineering.

Olivier, J. G., G. Janssens-Maenhout, M. Muntean, and J. A. H. W. Peters. 2016. "Trends in Global CO2 Emissions 2016 Report." PBL Netherlands Environmental Assessment Agency, The Hague.

Peters, B. "Additive Formwork: 3D Printed Flexible Formwork." Paper presented at the ACADIA 14: Design Agency, Los Angeles, California, October 2014.

Søndergaard, A., O. Amir, and M. Knauss. "Topology Optimization and Digital Assembly of Advanced Space-Frame Structures." Paper presented at the ACADIA 2013: Adaptive Architecture, Cambridge, Ontario, Canada, October 2013.

Veenendaal, D., M. West, and P. Block. 2011. "History and Overview of Fabric Formwork: Using Fabrics for Concrete Casting." *Structural Concrete* 12 (3): 164–77.

9 ACKNOWLEDGMENTS

The authors would like to thank a number of partners and collaborators whose dedication helped us fulfill the research discussed in this paper:

- Robert Flatt, Nicolas Ruffray, Timothy Wangler, Lex Reiter (Physical Chemistry of Building Materials Chair, ETH Zürich)
- Heinz Richner, Andreas Reusser (Concrete Lab, ETH I)
- Moritz Studer, Oliver Wach, Kathrin Ziegler, Felix Stutz, Neil Montague de Taisne, Curdin Tano (Bachelor Thesis, Engineering, ETH Zürich);
- Matthias Leschok, Ioannis Fousekis, Ma Xijie (Student Assistants, ETH Zürich)
- Mania Meibodi, Hyunchul Kwon, Rena Gieseke, Demetris Shammas, Pietro Odaglia, Ana Anton, and the rest of the DBT Chair
- Mariana Popescu (Block Research Group, ETH Zürich)
- Tanja Coray, Orkun Kasap (NCCR Digital Fabrication)
- Christian Specht, Moritz Begle, Stefan Schwartz (Industry Partners)
- Hannes Heller (Gramazio Kohler Research, ETH Zürich)
- The Concrete Canoe Club Zürich (Pirmin Scherer, Lukas Fuhrimann, Hannes Heller, Patrick Felder, Jonas Wydler, Jonas Henken, Andreas Näsbom, Anna Menasce, Caterina Rovati, Roman Wüst, Pascal Sutter, Thomas Rupper, Jonathan Hacker)
- This research was supported by the NCCR Digital Fabrication, funded by the Swiss National Science Foundation (NCCR Digital Fabrication Agreement #51NF40-141853).